SAR Image Quality Assessment

A.Martínez[1] and J.L.Marchand[2]
[1] *Inisel Espacio, Av.Burgos 8 bis, 3. 28036 Madrid - Spain*
[2] *On Board Data Handling Division. ESTEC - ESA P.O.Box 299, 2200 AG Noordwijk - The Netherlands*

RESUMEN

El análisis de calidad es una importante tarea desarrollo de métodos de procesado digital de genes SAR. En este artículo se presenta una metodología de análisis válida para blancos puntuales extensos. La utilidad de esta metodología se pone manifiesto en el estudio de dos casos prácticos: el enfoque correcto de las imágenes SAR y el efecto del ancho de banda procesado en las imágenes SAR;

PALABRAS CLAVE: procesado SAR, calidad.

ABSTRACT

Quality analysis is an important task in the development of SAR image digital processing methods. In this paper a methodology for the analysis of both point target and extended target in SAR images is presented. The utility of the proposed methodology is demonstrated in the study of two practical situations: the correct focusing of images and the of the processed bandwidth on SAR images.

KEY WORDS: SAR processing, quality analysis

INTRODUCCIÓN

The increasing interest of the Remote Sensing Community on Synthetic Aperture Radar (SAR) images during the past twenty years has made Digital SAR Data Processing an active field of research.

In contrast to optical imagery, SAR data have to be pre-processed in order to obtain an image. The focusing of SAR raw data is essentially a two dimensional problem. The reference function of this correlation is the Impulse Response Function of the SAR system. The most straightforward way to perform the compression is directly in the 2D time domain (Barber, 85). Due to the huge computational burden of this method, other approaches working in the frequency domain have been investigated in the past, being the most common procedures the range-Doppler and the wave domain, approaches.

The aim of these methods is to perform the 2D correlation as two ID correlations. The main problems arise from the azimuth compression, as the input data for correlation are located along range migration trajectories that are themselves range dependent

The main objective of the SAR quality analysis methods to be presented in this paper is to provide a tool for the study of the focusing performance of different processing algorithms and the influence of key parameters in the quality of the final image. They can also play an important role when studying the influence of common post processing techniques in SAR images, such as speckle filtering, geometric and radiometric calibration and data compression.

The definitions of the main SAR quality parameters are given in the second section of this work. The methodology used to conduct the analysis is presented in section three. Several examples of SAR quality analysis are discussed in the fourth section. Finally, the conclusion are summarized.

SAR QUALITY PARAMETERS

The SAR response to a point target, assuming negligible background reflectivity and thermal noise, is commonly referred to Impulse Response Function (IRF). The analysis of the signature of a point target in a SAR image allows the determination of several parameters that are related to the SAR spatial resolution and the presence and importance of undesired side lobe peaks. Also related with the SAR response to a point target is the ambiguity level, which measures the energy of the point target focused in different spatial points.

The radiometric resolution is obtained through the study of the variations of pixel values within an homogeneous area; that is, the statistics of the SAR response to a region with constant backscattering coefficient.

Peak intensity and amplitude

A SAR image is fue result of coherently processing retumed echo signals; thus, fue pixel values are complex quantities. For most applications fue representation of the magnitude of the image is enough. It is possible to use the modulus of fue complex pixel (amplitude) as well as the squared modulus (intensity). The peak intensity is fue maximum pixel value in fue main lobe of the impulse response function (if the image has been power detected). The square root of the intensity is the amplitude.

Spatial resolution

The spatial resolution is the distance between the points with intensities 3 dB bellow the maximum intensity of the main lobe peak in the azimuth and range directions. The definition of the - 3 dB points is equivalent to the points with half fue intensity of fue maximum:

$$[I_{max}]_{dB} = [I_{3dB}]_{dB} + 3$$
$$10\log_{10} I_{max} = 10\log_{10} I_{3dB} + 3$$
$$I_{max} / I_{3dB} = 10^{3/10} = 1.995262 \approx 2$$

It is sometimes useful to have parameters measuring the width of the main lobe at differences heights. We have made extensive use of the width at one tenth of the intensity of the maximum (that is, an intensity 10 dB bellow the maximum) and algo of fue distance between the first two minima of the main lobe, both in range and azimuth directions. See figure 1 for a graphical representation of these parameters.

Peak side lobe ratio

The peak side lobe ratio, PSLR, is defined as the ratio of the peak intensity of the most prominent side lobe to the peak intensity of the main lobe. There are tour measures of the PSLR, corresponding to the two sides of the main lobe both in azimuth and range directions. Usually, the largest of the two sides for a given direction is finally reported, and this parameter is expressed in decibels.

Unfortunately, there is not a simple procedure to decide wether a peak is a true secondary lobe or not. For this reason, it is convenient to report the two computed PSLR's corresponding to the first maximum (that closest to the main lobe) and to the absolute one.

Integrated side lobe ratio

The integrated side lobe ratio, ISLR, is the ratio of the power (energy) in the main peak to the total power in all the side lobes (or vice versa, depending on definition). As for the PSLR, the ISLR is a measurement of the relative importance of fue sirle lobes with respect to the main lobe. This parameter is usually expressed in decibels. There are several definitions of the ISLR in the literature, with the difference in the adoption of the areas in which the energy is integrated:

(Sánchez, 91) ISLR is the ratio of the energy inside a rectangle centred on the maximum of the main lobe and side length equal to the - 3 dB width of the IRF to the rest of the energy of the IRF. In this definition, only one resolution cell is considered to have the energy in the main lobe.

$$ISLR = 10\log \frac{\int_{-3dB} Idxdy}{\int_{-\infty}^{10+\infty} Idxdy - \int_{-3dB} Idxdy} \qquad (1)$$

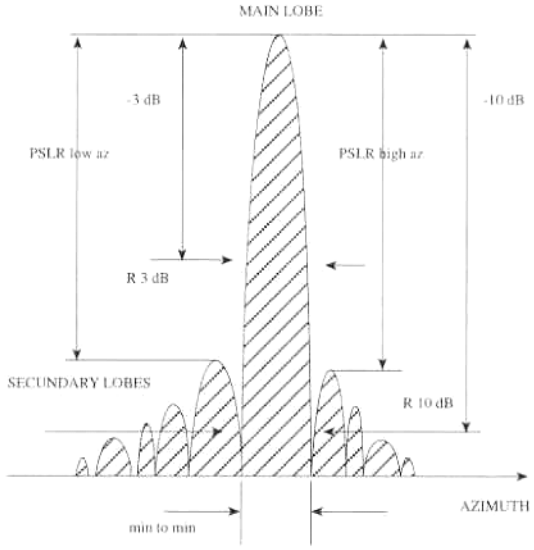

Figure 1. Graphical representation of a SAR point target showing several quality parameters.

(Franceschetti,91) They define the normalized integrated side lobe ratio, NISLR, as follows:

$$NISLR = I_{max} 10\log_{10} \frac{\int_{-\infty}^{+\infty} Idxdy}{\int_{-\infty}^{+\infty} Idxdy - \int_{-3dB} Idxdy} \qquad (2)$$

(Guignard, 79) There are three different regions in fue IRF: the main bearn afea, which is 3 by 3 pixels centred on the maximum; fue guard band, which is formed by the 26 pixels surrounding the main beam afea; and the side lobe afea, formed by a square of 99 pixels side, disregarding the inner 5 by 5 window.

$$ISLR = 10\log_{10} \frac{\int_{99x99} Idxdy - \int_{5x5} Idxdy}{\int_{3x3} Idxdy} \qquad (3)$$

(Holm, 91) Ratio of the power within a square centred on fue maximum and twenty by twenty resolution cells, without considering an inner window of three resolution cells side and the power in the second window.

$$ISLR = 10\log_{10} \frac{\int_{20x20} Idxdy - \int_{3x3} Idxdy}{\int_{3x3} Idxdy} \qquad (4)$$

(ESA, 90,91) Ratio of fue power within a square centred on the maximum and ten resolution cells side, without considering an inner window of two resolution cells side and the power in the second window.

$$ISLR = 10\log_{10} \frac{\int_{10x10} Idxdy - \int_{2x2} Idxdy}{\int_{2x2} Idxdy} \qquad (5)$$

The ESA' s definition will be used in this work, along with a normalized ISLR defined as follows:

$$\text{normISLR}=10\log_{10}\frac{\frac{1}{96}(\int_{10x10}\text{Idxdy}-\int_{2x2}\text{Idxdy})}{\frac{1}{4}\int_{2x2}\text{Idxdy}} \quad (6)$$

Ambiguity level

There are two types of ambiguities in SAR: the range ambiguities, which results from the simultaneous arrival of different pulses at the antenna, and the azimuth ambiguities. The range ambiguities are controlled via the PRF (Pulse Repetition Frequency) selection. On the other hand, azimuth ambiguities are produced by the finite sampling of the azimuth frequency spectrum at the PRF.

During the processing of SAR raw data, a selection of the frequency bandwidths has to be performed. As the process is made in digital form, care has to be exercised to avoid any violation of the Nyquist sampling criterium. This criterium establishes that the maximum frequency of a signal that can be processed is just half the sampling rate. In the case of SAR images, the higher frequency contents of a point target can be focused in a different spatial location than the Test of the frequencies if the processed azimuth bandwidth is too broad. These artifacts are called ghosts in the literature.

The ambiguity level is the ratio of the energy in the ghosts to that in the main lobe, and is expressed, in dB.

Radiometric resolution

The radiometric resolution of a SAR image is defined by the equation (Miller, 81):

$$\text{RadRes}=10\text{logl0}[1+\frac{\sigma}{\mu}] \quad (7)$$

where μ and σ are the mean value and standard deviation of the extended target intensity values.

METHODOLOGY

The measurement of the radiometric resolution is easily performed by extracting an homogeneous area from the original SAR image and calculating the statistics. The procedure for the analysis of point targets is somehow more elaborate, and is described bellow. An overview of the procedure is presented in figure 2.

Extraction of point targets

The calculation of the quality parameters of an image is not a straight forward task, at least in the case of point targets. Firstly, the target has to be extracted from the rest of the image before any analysis can be done. The reason for it is to avoid

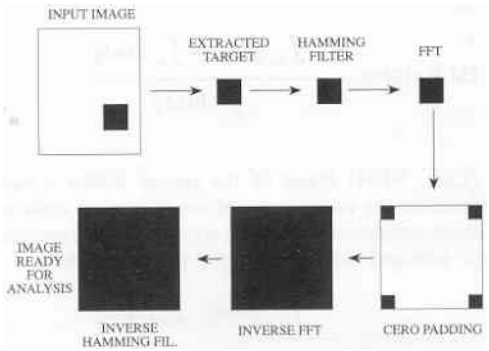

Figure 2. Point target analysis methodology

spurious influences of the surrounding environment. The point target should be as bright as possible, to improve the statistics. The preferable targets are man-made transponders and reflectors, but they are not available in most of the images; in this situation, opportunity targets can be used.

Interpolation

When analyzing a point target for impulse response function parameters determination, it is desirable to have an interpolated image to perform the calculations. In this way, the obtained parameters will be more accurate than in the case when no interpolation is done. The interpolation is made via a FFT zooming method with complex data (Fraser, 89; Cavichi, 92).

As we will be using Fourier transforms, the input data should be converted to complex formal in the case they were real; this is done by adding a null imaginary part and changing the pixel formal to float. The next step in the zooming is a Hamming window filtering of the input image in order to prevent side effects in the Fourier transforms. Then, the two dimensional Fourier transform of the filtered image is performed to obtain the point target spectrum. The zooming is a delicate task that should be handled with care due to the noisy nature of the SAR signal. The use of smoothing filters is mandatory before the calculation of maximum or minimum values of the spectrum.

The Fourier spectrum is divided in tour equal quadrants. These quadrants are put in the corners of a bigger spectrum, with the size of the desired interpolated image by padding with zeros the central area. At this point an inverse Fourier transform is calculated. The last step in the formation of the interpolated image is to remove the effects of the Harnming window filtering, although it is not necessary.

Evaluation of quality parameters

Once the interpolated image is available we are in position to calculate the different quality parameters. The search for secondary lobes mar not be restricted to the range and azimuth directions alone. Sometimes it can be interesting to search for

a possible deviation of the secondary lobes from the range and azimuth directions. This angular drift can be related to any inhomogeneity in the SAR processor kernel.

Additionally, the position of both the first secondary lobes (those closest to the main peak) and the absolute ones in the extracted image have to be obtained. The accuracy of the spatial resolution is improved by using linear interpolation of the pixel values; in this way, subpixel precision can be achieved.

Implementation notes

The proposed methodology was first implemented in three independent programs:

extract for the extraction of targets
interpol for the point target interpolation
quality for the parameters estimation

Additionally, a program for the conversion of the complex interpolated target images into one byte per pixel format (for displaying purposes) was developed.

The routine execution of the quality software is somehow troublesome, as it includes different programs with more than twenty input parameters. The use of shell scripts (UNIX command procedures files) can ease a little this task, but when one is embarked with a great number of tests, they are not the solution.

In order to avoid this problem, the zooming procedure has been implemented in a standard image display tool, **cidvisu**, developed at WDP-ESTEC (Armbruster, 1992). In this environment you select a point target with the cursor and press the mouse middle button; then, a menu panel for inputting the zooming parameters appears on the screen. Once the proper parameters have been entered the extraction, interpolation, modulus detection and display of the target are done automatically.

EXAMPLES OF QUALITY ANALYSIS

The developed programs have been tested in order to assess their performance and also to estimate the minimum zooming factor needed to obtain accurate results. The analysis of the results shows that the precision of the parameters is improved when increasing the zooming factor of the interpolated image. Detailed description of these tests can be found in (Martínez, 92) and (Dendal, 92).

Description of the test image

The test has been made with ERS-l SAR raw data from the Flevoland test site (The Netherlands) acquired on October 25th 1991. In this area there are three transponders and several comer reflectors deployed, that are and have been used for the calibration of the microwave equipment on board ERS-1 (Desnos, 91). The processing of the raw data was performed with a CSA SAR processor, developed jointly by ESTEC and Inisel Espacio (Martínez, 93).

Focused versus unfocused images

The first example we are presenting comprises the evaluation of the focusing performance of a SAR processor. For this test we have choosen an area centered at the transponder number two (Vliegveld), and have made two runs of the CSA processor. In the first run, the Doppler parameters used had the correct values, so the resulting image is well focused (the three looks image is shown in figure 3). Then, we changed slightly the value of the FM rate (0.2% of the true value) and made the second trial. The corresponding three looks image is shown in figure 4. The bright spot at the top center of the images is the transponder.

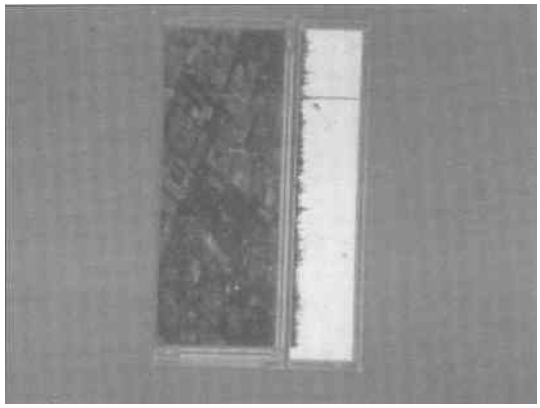

Figure 3. Well focused 3-looks image Flevoland area near transponder number 2

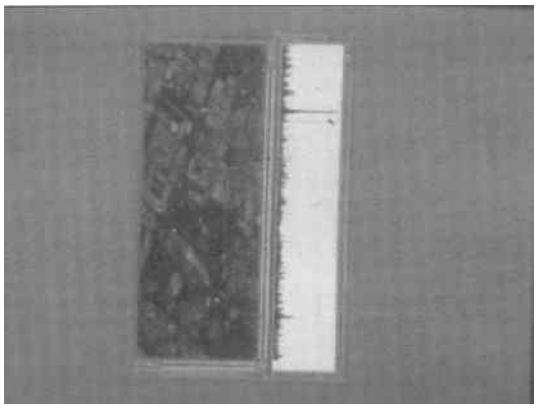

Figure 4. Badly focused 3-looks image Flevoland area near transponder number 2

The visual inspection of the two images shows very little difference between them, as both appears to be well focused. At this point we performed the point target analysis of the transponder. In figure 5 and 6 we present the transponder zoomed by a factor 8 from the single look complex images obtained before, as well as the profiles in the range and azimuth directions. Now it is easy to note the differences between the two images:

- There is no change between the images in the range (horizontal) direction, as the FM rate mismatch only affects the focus in the azimuth (vertical) direction.
- The degradation of the quality of the point target corresponding to the wrong FM rate is reflected in the broadening of the main lobe in the azimuth direction. Note also that the secondary lobes, clearly visible in the well focused image, are joined to the main lobe in the badly focused image.
- The Impulse Response Function of the first image is more concentrated around the central point.

The quality analysis of the zoomed targets allows the quantification of the previous comments. The main results (spatial resolution, one tenth width, PSLR and ISLR) are listed in table l. All these results were obtained from the single look complex images.

While the parameters measured in the range direction are equivalent, there is a significative difference in those corresponding to the azimuth direction, as commented before. The ISLR is also affected by the focusing, as it contains information of the whole IRF. It is interesting to point out the bigger relative increase in the one tenth width value than the corresponding to the spatial resolu tion (one half width).

	AZIMUTH			RANGE		
	Sp res (m)	1/10 width m	PSLR (dB)	Sp res (m)	PSLR (dB)	ISLR (dB)
Well focused	4.14	7.08	-20.3	8.60	-13.0	-10.1
Badly focused	5.29	12.89	-17.9	8.62	-13.0	-7.4

Table 1. Comparison of quality parameters of well and badly focused point target

Ghosts in SAR images

We will examine in this example the effect of the processed azimuth bandwidth on the point target response. The two images to be compared were taken from a region around the transponder number 1 (Pampus-hout). The first one was processed using the full azimuth bandwidth (1678.712 Hz) while in the second only 1000 Hz were used. All other processing parameters were kept constant. The tour looks images are shown in figures 7 and 8 respectively. Note the presence of the transponder as a bright cross at the center of the images. The bright area on the right of the transponder is a small city.

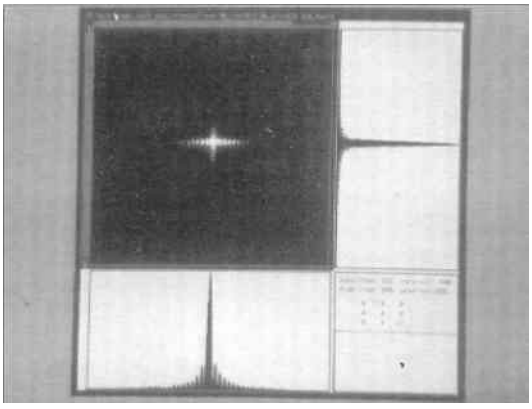

Figure 5. Well focused, interpolated l-look image of transponder number 2 (zoom factor: 8).

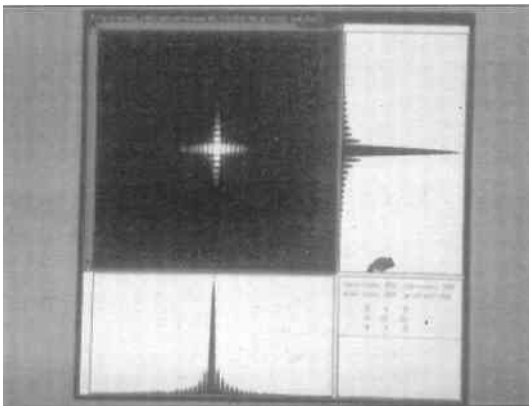

Figure 6. Badly focused, interpolated l-look image of transponder number 2 (zoom factor: 8).

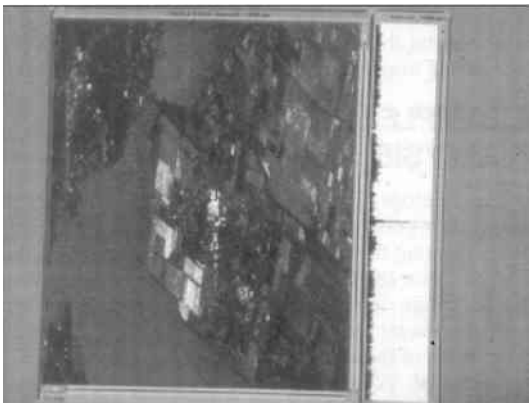

Figure 7. 4-looks image of Flevoland area near transponder number l. Processed azimuth bandwidth: 1678.712 Hz.

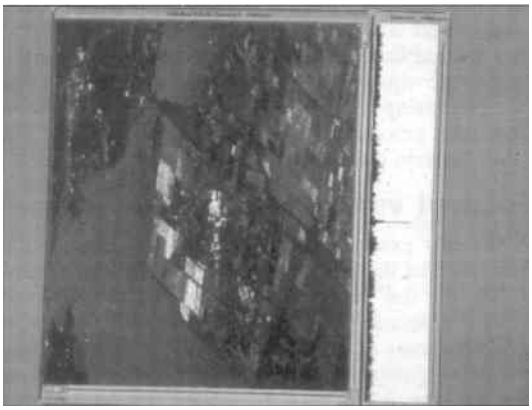

Figure 8. 4-looks image of Flevoland area near transponder number 1. Processed azimuth bandwidth: 1000 Hz.

	AZIMUTH				
	Sp resol (m)	1/10 width (m)	min to min (m)	PSLR (dB)	Ambiguity Level (dB)
Azimuth band 1679. Hz	4.17	7.12	9.95	-19.6	-22.3
Azimuth band 1000. Hz	6.23	10.49	14.42	-15.3	-28.0

Table 2. Comparison of qua1ity parameters of images processed with different bandwidths

At first sight the two images are the same. However, a close inspection of figure 7, the one from the full azimuth bandwidth, reveals the presence of bright features at the top of the image, in a water area and surroundings. These features does not appear in figure 8, and are ghost images of the bright urban area and the transponder. In the processing of the 1000 Hz image, the higher frequency contents were ignored, producing lower ambiguity in the azimuth direction.

To calculate the ambiguity level, we have to locate the ghost images of a given target. Those corresponding to the transponder in the full bandwidth image can be observed at the same horizontal position and near the top and bottom of the image. The great backscattering coefficient of the transponder enables the localization of the ghosts. For the 1000 Hz image it is much more difficult to distinguish the ghosts. The ambiguity level is obtained from the difference of the energy (intensity) in the point target and in the ghosts. As can be seen in table 2, the broader the processed bandwidth the higher the ambiguity level.

On the other hand, the reduction of the bandwidth has negative effects on the point target response. The interpolated point targets corresponding to the full and 1000 Hz bandwidth images are shown in figures 9 and 10. After a fast look at the figures, it is clear that the reduction of the bandwidth produces a broadening of the IRF. The main quality parameters (including the minimum to minimum width) in the azimuth direction are listed in table 2. However, the shape of the IRF is not distorted, as was the case with the unfocused image of the previous example.

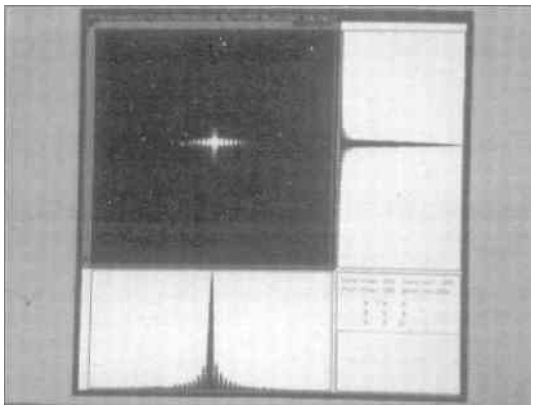

Figure 9. Interpolated l-look image of transponder number 1 (processed azimuth bandwidth: 1678.712 Hz; zoom factor: 8).

It is interesting to compare the width of the main lobes of the unfocused and the 1000 Hz images (although they come from different targets). The spatial resolution is better for the former (5.29 vs. 6.23 m), as it is less affected by the distortion of the IRF. Nevertheless, the -10 dB width (12.89 vs. 10.49 m) and the minimum to minimum width (21.88 vs. 14.42 m) reflect clearly the distorted shape of the unfocused image.

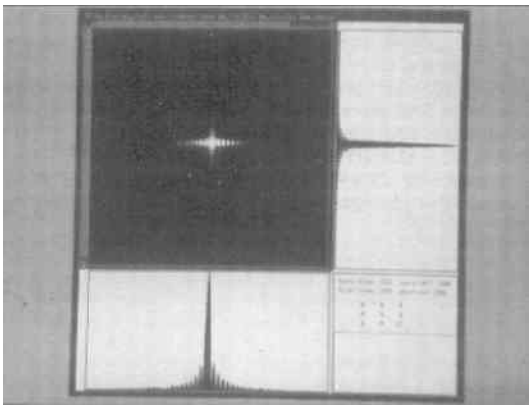

Figure 10. Interpolated 1-look image of transponder number 2 (processed azirmuth bandwidth: 1000. Hz zoom factor: 8).

CONCLUSIONS

The calculation of quality parameters of SAR imagery is an important task that has applications in the assessment of both the sensor hardware and the processing software. The performance characteristics of SAR imagery allows the users to know if the products specifications match their own requirements.

The proposed methodology for the quality analysis of SAR images has been applied to two practical examples. In both cases, the quality parameters allow the qualitative and quantitative analysis of the images. The visual inspection was shown to be of little help.

ACKNOWLEDGEMENTS

One of the authors (A.M.) wants to express his gratitude to R.Creasey, Head of the On-board Data Handling Division, ESTEC-ESA, for the opportunity to spend a fruitful one year stay at ESTEC. This work was supported by CDTI within the Spanish National Space Plan. All ERS-1 images used in this work are copyright of ESA.

REFERENCES

ARMBRUSTER, P. (1992). «Definition of a Cornrnon Image Descriptor (CID), Technical Specification ESTEC/WDP/ CIDV2.1.

BARBER. B.C. (1985). «Theory of digital imaging from orbital synthetic aperture radar», *Int. J. Remote Sensing* vol.6 1009-1057.

DENDAL. D. and MARCHAND J.L. (1992). «Ω-K techniques advantages and weaker aspects», en *Proc. IGARSS'92,* 366-368.

DESNOS, Y.L. (1991). «Point target analysis on UT169110250214028.El (ERS-I SAR image of Flevoland from 25.10.91», ESTEC internal memo.

ESA (1990). «Technical note on fue ECISAR test image». ER- TN-EPO-GP-1901, ESTEC-ESA.

ESA (1991). «ECISAR TEST IMAGE: quality analysis and calibrations measurements», ER- TN-EPO-GP-1902, ESTEC-ESA.

FRANESCHETTI G., LANARI R. and PASCAZIO V. (1991). «Wide angle SAR processors and their quality assessment», en *Proc. IGARSS'9I,* 287-290.

GUIGNARD, J.P. (1979). «Final acceptance of fue MDA software SAR processor», en *Proc. SEASAT SAR processor workshop,* ESA SP-154, 91-100.

HOLM S., VALAND P.A. and ELDHUSET K. (1991). «Performance of CESAR ERS-1 SAR processor», en *Proc. IGARSS'91,* 291-294.

MARTINEZ A. (1992). «Development of a SAR processing environment». ESA-ESTEC WDP/AML/1694.

MARTINEZ A. and MARCHAND J.L. (1993). «lmplementation and quality analysis of a CSA SAR processor». (accepted for presentation at IGARSS'93).

MILLER, P.P. (1981). «Measurement of radiometric criteria», en *Proc. SAR image quality workshop,* ESA SP-172, 33-40.

SANCHEZ J.I. (1991). «Software tools for quality measurement in SAR images», ESA-ESTEC-X-853.